

Evaluation of Two-Equations RANS Models for Simulation of Jet-in-Crossflow Problems

Srinivasan Arunajatesan¹ and Christopher W.S. Bruner²

Sandia National Laboratories, Albuquerque, NM 87185.

Results from an investigation of the predictive capabilities of various two-equation RANS models for the jet-in-cross flow problem are presented. The flow regime consists of a supersonic jet issuing into a transonic cross flow. The parameters varied are, the jet momentum ratio, jet inclination angle and cross flow Mach number. The goal of the investigation is to characterize the behavior of the turbulence models in this flow regime - this has implications for accurate predictions of vortex-fin interactions.

I. Introduction

Recent investigations on jet-fin interactions have shown that the effect of the induced flow angle at the fins due to the vortices generated by the jets is the main cause of the jet/fin interactions[1][2][3][5]. Prediction of this interaction and the resultant alteration of the force generated by the fins depend upon accurate prediction of the vortex locations with respect to the fins and their strengths. However, before predictions of the aerodynamic forces on fins and their modification by the vortices can be reliably made, a comprehensive understanding of the turbulence modeling required for such an effort is needed. This paper seeks to address this need by carrying out a detailed study on a related subscale problem, specifically targeting the effect of the turbulence modeling on the predictions of the vortex system induced by a jet in cross flow.

A large number of experimental and numerical studies of the jet in crossflow problem have been carried out and provide a good understanding of the features that dominate this flow field. In a time averaged sense, the flow field is dominated by the counter-rotating vortex pair (CVP) tracking the jet and the horse-shoe vortices (HSV) that wrap around the jet. Detailed time resolved measurements and LES simulations have also shown the presence of Kelvin-Helmholtz type instability generated vortices in the jet shear layers and vortices in the wake region. With regards to the jet/fin interaction problem, it has been demonstrated clearly [5] that this results from strong effects of the CVP and the HSV on the flow field in the immediate vicinity of the fins. The flow induced by these vortices alter the effective angle of attack on the fins, thereby modifying the pressure distribution on the fins and hence the force and moments generated by them.

Recently, several numerical predictions [7][8][9] of this flow field have been presented using Large Eddy Simulations. While these studies have demonstrated the ability to predict the flow field characteristics, no evaluations of their ability to predict jet/fin interactions have been presented. In addition, these simulations are still too expensive for calculations in a design environment and the use of RANS modeling is essential and unavoidable. Vortically dominated flows (wingtip, vortex-fin interaction, jet in cross-flow) have traditionally been difficult to accurately model using two-equation RANS models. Recently, modifications [10] and sensitization procedures [11] have been proposed to improve these predictions; however, the performance of these “improvements” for the jet/fin interaction predictions is not clear. Hence, understanding of the performance of RANS models for predicting quantities of interest to jet/fin interactions is crucial to successful predictions of the interaction problem.

In the present paper, we evaluate two-equation RANS models on a model jet-in-cross flow problem. This configuration has been studied extensively using experiments [2][3][4] and detailed measurements of the vortex locations, surface pressure distributions etc are available. Thus the problem is particularly well suited for a validation and evaluation exercise, such as the one pursued here.

¹ Principal Member of Technical Staff, Aerosciences Department, PO Box 0825, Senior Member AIAA.

² Principal Member of Technical Staff, Aerosciences Department, PO Box 0825, Associate Fellow AIAA.

II. Flow field configuration and Problem Setup

The configuration studied here corresponds to that studied experimentally by Beresh and Co-workers[2][3][4]. The setup consists of a supersonic jet issuing from the floor of a 12" x 12" test section in a blow down wind tunnel at Mach number of 0.8. The jet exhausts from a conical nozzle with a design Mach number of 3.73 and an exit diameter of 0.375". In the experiments, the nozzle orientation is varied from vertical to cant angles upto 45 degrees. Here we only use the 15 degree cant angle data. The nozzle is located on the floor of the test section and PIV measurements of the velocity field are available at a streamwise location that is 33.8 jet diameters downstream of the jet.

The flow conditions studied here correspond to one of the test conditions in Beresh et al [4]. The tunnel Mach number is 0.8 and the jet dynamic pressure ratio (denoted by J) is 10.2. The tunnel stagnation pressure is 154KPa and the jet stagnation pressure is 4.97 MPa. The stagnation temperatures are 320K for the tunnel and 300K for the jet, yielding a free stream velocity at the tunnel centerline equal to 286 m/s.

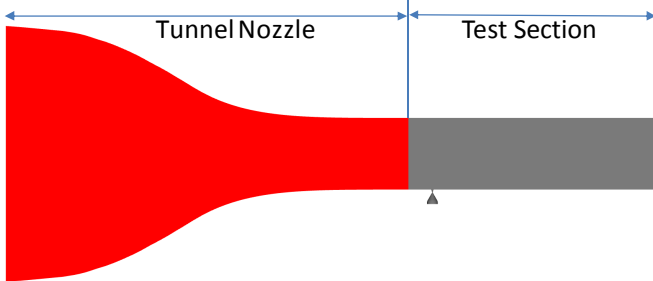


Figure 1. Simulation setup for the current work showing the tunnel nozzle and test section relative to the jet.

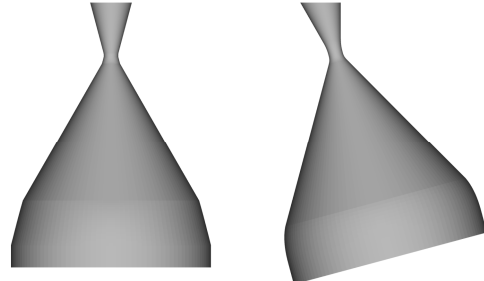


Figure 2. Jet nozzles used in the present simulations.

The overall simulation setup is shown in Figure 1. The test section sits at the end of a long nozzle section and therefore the boundary layer upstream of the jet location is thick compared to the jet exit diameter. In the present work, in order to account for this in a cost effective manner, the simulations have been performed in two steps. First a simulation of the wind tunnel nozzle including just the test section (no jet nozzle) is carried out. At a station corresponding to 10.66 jet diameters upstream the flow field variables are extracted and provided as boundary conditions to the jet in crossflow simulations including the jet. The computational domain corresponding to the jet in cross flow simulations is shown in grey in Figure 1.

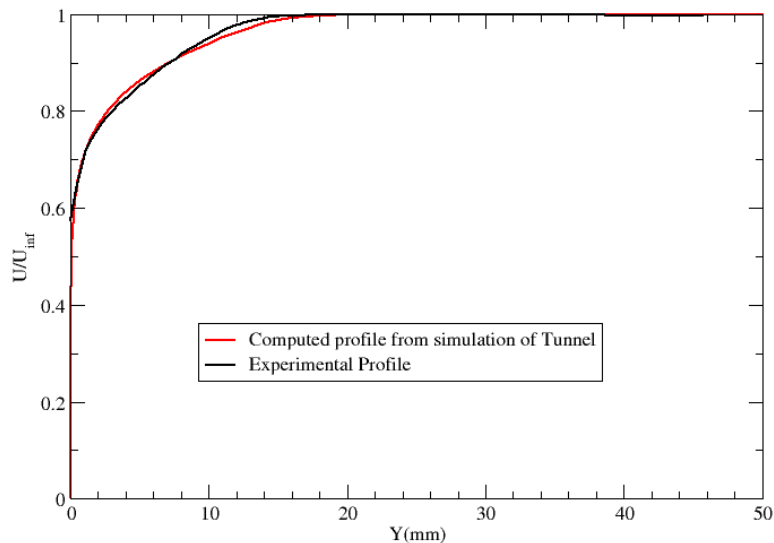


Figure 3. Comparison of the computed boundary layer profile with the measured data. The comparison is shown at a location $\sim 30D_j$ downstream of the jet.

As part of the experimental work, detailed measurements of the boundary layer was on the tunnel walls were carried out. The measurements however were made at a station corresponding to the PIV measurements,

downstream of the jet location. A comparison of the boundary layer profile with the measured profile at this location is shown in Figure 3. It is clear that the predicted profile agrees reasonably well with the measured profile. This provides some confidence that the inflow boundary condition used in the present work is representative of the experimental conditions.

The tunnel side walls and top walls are located 16 and 32 jet diameters away from the center of the jet exit. It is not expected that the tunnel boundary layers on these walls have a significant effect on the flow features; hence these are modeled as slip walls in the present work. The downstream boundary is located about 100 jet diameters away from the jet exit and is treated using a characteristics based non-reflective boundary condition.

As outlined above, the jet issues from a conical nozzle with an exit diameter of 0.375". In order to provide appropriate boundary conditions for the jet, the entire nozzle including the convergent portion is included in the present simulations. Stagnation condition boundary conditions are imposed on the jet upstream boundary corresponding to the experimental conditions. The jet nozzles for the vertical and canted cases are shown in Figure 2.

III. Flow Solver and Numerical Methods

The commercial software GASP (Version 4) [12] is used in the present work. GASP is a commercial CFD flow solver developed by AeroSoft, Inc. It solves the integral form of the time-dependent Reynolds-Averaged Navier-Stokes (RANS) equations in three dimensions. The solver is also capable of solving subsets of RANS equations, which include thin-layer Navier-Stokes, parabolized Navier-Stokes (PNS), the Euler equations, and the incompressible Navier-Stokes equations.

Steady state solutions can be marched in time using local time stepping. Time-accurate flows can be solved using either the dual-time stepping procedure, or an explicit Runge-Kutta algorithm. GASP supports multi-block, structured grid topologies. For complex geometries, Chimera/overset grids are supported with built-in hole-cutting and stencil selection. Several choices are available for inviscid fluxes, in the present work, we use standard Roe flux, the Roe flux.

To model turbulence, GASP has an array of options[13], only the two equation $k-\omega$ family of models is exercised in this work. These include Wilcox's 1998 [14] and 2006 variants[15] and Menter's SST model[16]. All calculations are run fully coupled with the primary conservation equations. For each of the models, simulations with and without compressibility corrections are carried out.

GASP uses message passing interface (MPI) in order to run on both shared and distributed memory platforms. GASP provides users with semi-automated domain decomposition in order to take full advantage of the parallel capability. For both single and multi-processor jobs, GASP supports full implicit time integration.

The computational mesh used in the present work consists of 10.5million cells in a block structured topology. Special care is taken to resolve the jet shear layer and near field wake region. In this abstract only the solution on this mesh is shown, simulations on finer and coarser meshes, demonstrating mesh convergence will be included in the final paper.

IV. Results and Discussion

As outlined earlier, simulations of a vertical and a canted jet have been carried out. Here we present a discussion of the results from these simulations. For clarity, the two cases are discussed separately.

A. Vertical Jet Cases

The general flow structure is illustrated in Figure 4(a), where contours of Mach number are plotted on a plane through the jet and wind tunnel centerline. The plots shown here are from the results of the simulation using the SST turbulence model, however, the general nature of the flow field is similar for all the cases. The over-expanded jet goes through a series of shocks and is turned by the tunnel flow. The Mach number contours clearly show the shock system that is formed. In addition the incoming boundary layer and the shear layer surrounding the jet core are also clearly visible. The wake region sees a separation that extends only a few jet diameters downstream and is closed by the expanding tunnel flow around the jet. The momentum exchange between the jet and the free stream is determined by the spreading of the shear layer in this near field, which in turn is a strong function of the turbulence model used. In general the extent of the turning of the jet determines the vertical location of the CVP and this in turn determines the extent of the jet/fin interaction downstream.

The vortical structure generated by the jet is illustrated in Figure 4(b). The CVP and the HSV are clearly visible in this plot. As mentioned above the CVP tracks the jet, in general sitting just within the extents of the jet plume itself.

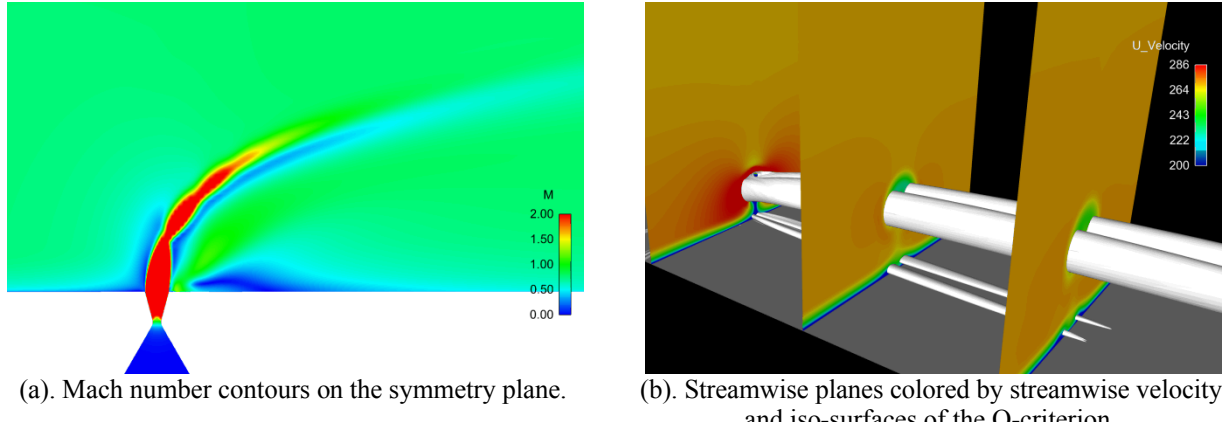


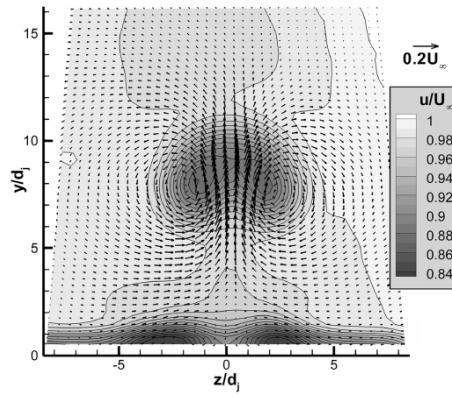
Figure 4. General features of the flowfield.

A detailed discussion of the results of the simulations will be presented in the final paper – only a brief discussion of the results to illustrate the differences observed between the predictions of the different turbulence models is presented here. A comparison of the cross plane velocity field predicted using the various models at a location $33.8D_j$ downstream with the measured velocity field is shown in Figure 5. The experimentally measured velocity field is shown in Figure 5(a). The figures (b)-(g) show the results for the three turbulence models ($k-\omega$ 1998, $k-\omega$ 2006 and SST); results with and without compressibility correction are included. The simulation using the $k-\omega$ 2006 model with compressibility correction was not stable and hence a steady solution could not be obtained for this case. In these figures, the contours show the streamwise velocity deficit in the jet plume, while the vectors show the flow in the cross plane, in particular the location of the vortices relative to the jet.

All the models capture the general nature of the flow field, the streamwise velocity deficit has the general shape seen in the measurements and the CVP, as seen in the vector plots are located “underneath” the jet, just within the extents of the plume. However a quantitative evaluation of the results shows that there are major differences between the predictions of the different models and with the experimental results. In general, the cases with the compressibility correction on predict a higher location of the jet plume and the vortex from the floor of the tunnel. The compressibility correction is predominantly active in the initial jet shear layer and tends to dampen the eddy-viscosity in this region. Thus the diffusion of the momentum due to turbulence is altered and this results in a difference in the jet trajectory downstream.

The cases with the compressibility off show better agreement of the jet location with the measured data. The $k-\omega$ 2006 model in general appears to be less diffusive than the other models. This model yields a solution that is not steady – the CVP continuously oscillates across the symmetry plane. The SST model and the $k-\omega$ 1998 model show significantly better agreement with the measured data. The SST model in general captures both, the location of the jet plume and the strength of the velocity deficit better. The $k-\omega$ 1998 model predicts a slightly higher location of the vortex and a greater strength for the velocity deficit.

From this discussion it is clear the best predictions for the cross-plane structure are obtained with the SST model without any compressibility correction.



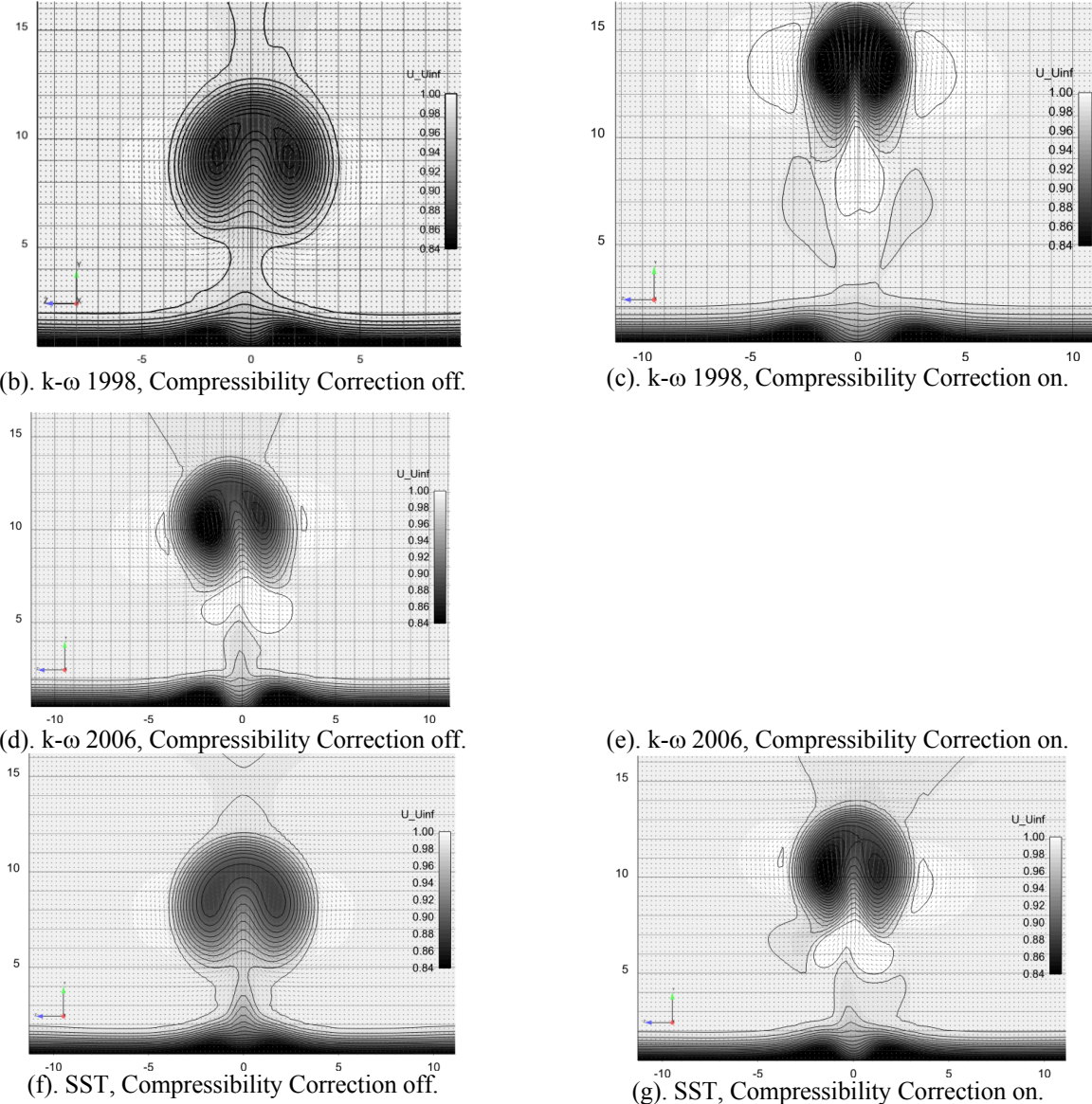


Figure 5. Comparison of the predicted velocity fields at a streamwise plane $33.8D_j$ downstream of the jet for the various turbulence models.

B. Canted Jet Cases

A similar assessment of the results for the canted case (as presented for the vertical jets above) is presented in Figure 6. Here again the cross plane velocity field at a location $33.8D_j$ downstream is shown and compared to the experimentally measured flow field. Here, due to the cant of the jet an asymmetry in the flow field is observed. Both the CVP and the HSV are both asymmetric with one of the vortices of the pair being slightly stronger than the other.

Again all the model predictions show generally the same features as the experiments. However, in all the cases, both, the location of the jet plume and the strength of the velocity deficit are not predicted correctly. In addition, the general shape of the jet plume is not captured very well either. The effect of the compressibility corrections in this case is not as clear as in the vertical jet case. The SST model with compressibility off which yielded the best results in the vertical jet case over predicts the size of the HSV, so much so that there appears to be an interaction between the CVP and the HV. The $k-\omega$ 1998 model with compressibility off, appears closer to the experimental measurement, though the size of the HSV and the strength of the velocity deficit are again over-predicted. Thus none of the models show satisfactory predictive capability for the canted jet case.

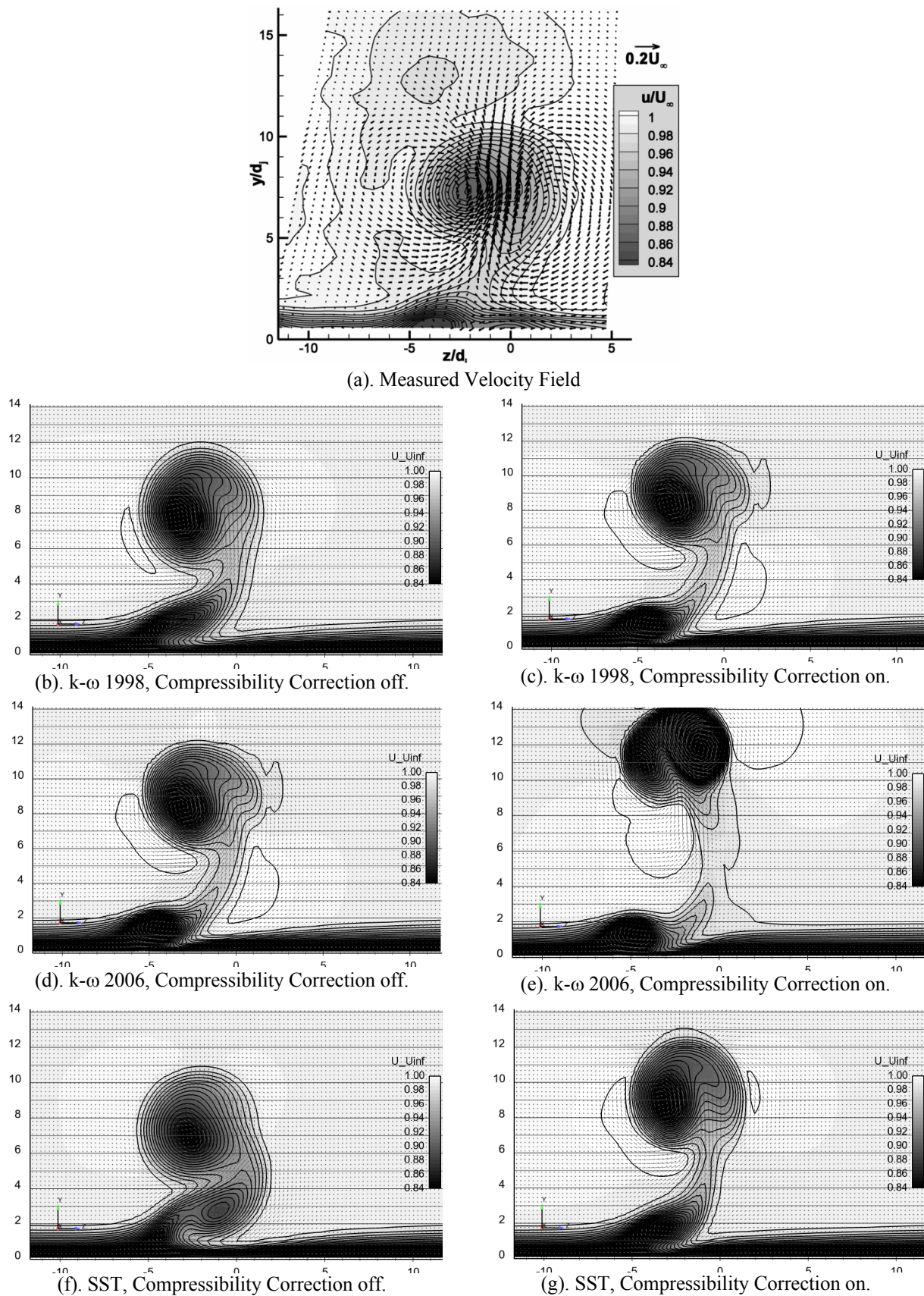


Figure 6. Comparison of the predicted flowfield with measured flow field for the canted jet case.

V. Summary and Final Paper Outline

Based on the above observations, it is clear that the predictive capabilities of the $k-\omega$ family of models examined here for the jet-in-cross flow problem are marginal at best. While the SST and $k-\omega$ 1998 models show promise for the vertical jet cases, the canted jet case predictions are very poor.

Due to space constraints, several details have been omitted here for brevity. The final paper will include a more complete description of the equations for the models examined in this work. A comprehensive analysis of the flow features associated with the various model predictions will be included and we will identify the reasons for the discrepancies in the predictions of the various models. Results from a detailed mesh refinement study, currently underway will also be included. In addition, we plan to also include additional two-equation models ($k-\epsilon$ models) within the scope of this study, results from these will also be included in the final paper.

VI. References

- [1] Peterson, C. W., Wolfe, W. P., and Payne, J. L., "Experiments and Computations of Roll Torque Induced by Vortex-Fin Interaction," AIAA Paper 2004-1069, Jan. 2004.
- [2] Beresh, S. J., Henfling, J. F., Erven, R. J., and Spillers, R. W., "Crossplane Velocimetry of a Transverse Supersonic Jet in a Transonic Crossflow," AIAA Journal, Vol. 44, No. 12, 2006, pp. 3051–3061.
- [3] Beresh, S. J., Henfling, J. F., Erven, R. J., and Spillers, R. W., "Penetration of a Transverse Supersonic Jet into a Subsonic Compressible Crossflow," AIAA Journal, Vol. 43, No. 2, 2005, pp. 379–389.
- [4] Beresh, S. J., Henfling, J. F., Erven, R. J., and Spillers, R. W., "Vortex Structure Produced by a Laterally Inclined Supersonic Jet in Transonic Crossflow", Journal of Propulsion and Power, Vol. 23, No. 2 2007, pp 353-363.
- [5] Beresh, S.J., Heineck, J.T., Walker, S.M., Shairer, E.T., and Yaste, D.M., "Planar Velocimetry of Jet/Fin Interaction on a Full-Scale Flight Vehicle Configuration", AIAA Journal, Vol. 45, No. 8, 2007, pp1827-1840.
- [6] Santiago, J. G., and Dutton, J. C., Velocity Measurements of a Jet Injected into a Supersonic Crossflow, Journal of Propulsion and Power, Vol. 13, No. 2, 1997, pp. 264–273.
- [7] Genin., F., Menon., S., 2010, "Dynamics of sonic jet injection into supersonic crossflow", J. Turbulence, 11:1-13, 2010.
- [8] Kawai, S. and Lele, S. K., "Dynamics and mixing of a sonic jet in a supersonic turbulent crossflow", Center for Turbulence Research Annual Research Briefs, 2009.
- [9] X. Chai and K. Mahesh., "Simulations of high speed turbulent jets in crossflow", AIAA Paper 2011-650.
- [10] Dechant, L.J., "Modifications to the $k-\omega$ Turbulence Model for Vortically Dominated Flows", AIAA Paper 2011-0056.
- [11] Spalart, P.R. and Shur, M., On the Sensitization of Turbulence Models to Rotation and Curvature, *Aerospace Science and Tech.* Vol. 5, 297-302, (1997).
- [12] GASP 4.0 User Manual , AeroSoft, 2002, ISBN 09652780-5-0.
- [13] Neel, R.E., Godfrey, A.G., Slack, D.C., "Turbulence Model Validation in GASP Version 4", AIAA Paper 2003-3740.
- [14] Wilcox, D. C., "Turbulence Modeling for CFD", DCW Industries, 2nd ed., 1998.
- [15] Wilcox, D. C., "Reassessment of the Scale-Determining Equation for Advanced Turbulence Models," AIAA Journal , Vol. 26, No. 11, 1988, pp. 1299–1310.
- [16] Menter, F. R., "Zonal Two Equation $k-\omega$ Turbulence Models for Aerodynamic Flows," AIAA Paper 93-2906, Jul. 1993.